Relative Reaction Rates of HCHO, HCDO, DCDO, $H^{13}CHO$, and $HCH^{18}O$ with OH, Cl, Br, and NO_3 Radicals

Karen L. Feilberg,*,† Matthew S. Johnson,† and Claus J. Nielsen‡

Department of Chemistry, University of Copenhagen, Universitetsparken 5, DK-2100 Copenhagen OE, Denmark, and Department of Chemistry, University of Oslo, Pb. 1033-Blindern, 0315 Oslo, Norway

Received: April 16, 2004; In Final Form: June 22, 2004

Formaldehyde (HCHO) is a principal intermediate in the photochemical oxidation of hydrocarbons in the troposphere. Isotopic analysis is an important tool for tracing the atmospheric path of gaseous species, and for this purpose, characterization of the isotope effects in the loss processes for formaldehyde is needed. The main loss pathways for formaldehyde in the atmosphere are photolysis and reactions with the radical species of OH, Cl, Br, and NO_3. In this study, the kinetic isotope effects in the reactions of five different isotopomers of formaldehyde (HCHO) with OH, Cl, Br, and NO_3 radicals are studied in a relative-rate experiment at 298 ± 2 K and 1013 ± 10 mbar. The reaction rates of DCDO, HCDO, $H^{13}CHO$, and $HCH^{18}O$ with the four radicals are measured relative to H_2CO in a smog chamber using long-path FTIR detection. The experimental data are analyzed with a nonlinear least-squares spectral-fitting method using measured high-resolution infrared spectra and cross sections from the HITRAN database. The reaction rates of HCDO and $HCH^{18}O$ with OH and Cl are determined relative to HCHO as $k_{OH+HCHO}/k_{OH+HCDO} = 1.28 \pm 0.01$, $k_{OH+HCHO}/k_{OH+HCH^{18}O} = 0.967 \pm 0.006$, $k_{Cl+HCHO}/k_{Cl+HCDO} = 1.201 \pm 0.002$, and $k_{Cl+HCHO}/k_{Cl+HCH^{18}O} = 1.08 \pm 0.01$. The reaction rates of HCDO and $HCH^{18}O$ with Br and NO_3 are determined relative to HCHO as $k_{Br+HCHO}/k_{Br+HCDO} = 3.27 \pm 0.03$, $k_{Br+HCHO}/k_{Br+HCH^{18}O} = 1.275 \pm 0.008$, $k_{NO_3+HCHO}/k_{NO_3+HCDO} = 1.78 \pm 0.01$, and $k_{NO_3+HCHO}/k_{NO_3+HCH^{18}O} = 0.98 \pm 0.01$. The errors represent 2σ from the statistical analyses, and do not include possible systematic errors.

Introduction

Formaldehyde (HCHO) is one of the most important carbonyl compounds in the lower atmosphere. It is present in both polluted and remote areas. It is produced from the combustion of fossil fuels, the photochemical oxidation of methane and other hydrocarbons, biomass burning, and microbiological processes. The decomposition of HCHO plays a significant role as a source of HO_x radicals throughout the atmosphere. About 40% of the CO source in the atmosphere stems from the oxidation of methane by OH via formaldehyde.[1] While the largest global photochemical source of HCHO is CH_4 oxidation, direct emission is typically the dominating source in and near urban areas. In certain regions with high emissions of non-methane hydrocarbons, such as isoprene (C_5H_8), the photochemical oxidation of these compounds can dominate HCHO formation.[2] Average mixing ratios of HCHO in the remote atmosphere are on the order of 10−100 ppt; in polluted areas, they may even reach 1−20 ppb.[3] The sources and sinks of formaldehyde in the atmosphere and their relative importance are not well-characterized. In particular, the roles of transport, heterogeneous chemistry, and halogen reactions are uncertain.[4] Recent airborne measurements of HCHO and other atmospheric species in the marine boundary layer and the upper troposphere have shown that HCHO concentrations in these areas are significantly higher than current models predict.[5,6] This suggests that the HO_x source from HCHO in these areas is greater than previously thought, and that unknown sources of HCHO are present in the upper troposphere.

The main loss pathways for formaldehyde in the troposphere are photolysis, reactions with radicals, and deposition.[2,7] Photolysis and the reaction with OH (the lifetime of HCHO with respect to OH is about 24 h)[8,9] compete during the day; the reaction with Cl (the lifetime of HCHO with respect to Cl is about 2 months)[9,10] is important in the marine boundary layer, and the reaction with the nitrate radical is the dominant loss process for HCHO at night (the lifetime of HCHO with respect to NO_3 is about 9 years). The reaction with chlorine can dominate HCHO loss, and thereby the isotopic signature, in the marine boundary layer where concentrations are sometimes very high. Aldehyde reactions (HCHO and CH_3CHO) have been identified as the most important sink for Br atoms during ground-level ozone depletion events in the Arctic marine boundary layer.[11] The reaction of HCHO with Br can also be a significant sink for ozone-destroying Br atoms in the stratosphere.[11,12] Characterization of the isotope effects in the loss processes for formaldehyde is an important step in tracing the carbon, hydrogen, and oxygen isotopic signatures in the processes throughout the methane oxidation mechanism.[13]

Recently, the deuterium isotope effect in the reactions and photolysis of formaldehyde have generated a great deal of interest because the photolysis of HCDO is the main source of atmospheric HD.[14] Molecular hydrogen is the basis of new fuel-cell technologies that may replace fossil fuels; however, the global budget of H_2 and the effect of an increase in its mixing ratio are not well-understood.[15−17] Measurements of D/H ratios can help to constrain sources and sinks of atmospheric H_2; however, the isotopic signature of the largest source of H_2 (the oxidation of methane via HCHO) has not been fully characterized.[14] The photolysis of HCHO is the only route transferring the hydrogen isotope signature in methane and non-methane

* Corresponding author. E-mail: klf@kiku.dk.
† University of Copenhagen.
‡ University of Oslo.

10.1021/jp048329k CCC: $27.50
Published on Web 08/12/2004

hydrocarbons to H_2.[14] The deuterium enrichment in formaldehyde is determined by the kinetic isotope effects (KIEs) in the reactions that produce it, the enrichment in the precursor hydrocarbons, and the KIE of the chemical reactions of formaldehyde. The relative reaction rates of HCHO and HCDO with atmospheric radical species, particularly OH and Cl, are thus important factors in assessing the budget of H_2. Although the societal relevance of the present study is linked to environmental issues, the reactions of HCHO with OH, Cl, Br, and NO_3 present some kinetic features that are of theoretical interest.[18,19] In this study, we present the reaction rates of four isotopomers of HCHO (DCDO, HCDO, $H^{13}CHO$, and $HCH^{18}O$) with OH, Br, Cl, and NO_3 radicals relative to the most abundant isotopomer. We have previously shown that these reactions exhibit large hydrogen kinetic isotope effects (KIEs) for DCDO ranging from 30% for Cl to 750% for Br, while the ^{13}C KIEs are on the order of 3−10%.[18−20] The $k_{OH+HCHO}/k_{OH+HCDO}$ KIE has previously been studied by mass spectrometry,[21] and the $k_{Cl+HCHO}/k_{Cl+DCDO}$ and $k_{OH+HCHO}/k_{OH+H^{13}CHO}$ KIEs have been studied by FTIR spectroscopy.[22,23] The present study extends the previous studies of isotope effects in the radical reactions of atmospheric aldehydes to include measurements for HCDO and $HCH^{18}O$.

Experimental Section

The kinetic study was carried out by the relative-rate method in a static gas mixture, in which the decays of the concentrations of the reacting species are measured simultaneously as a function of reaction time. Consider two simultaneous bimolecular reactions with the rate coefficients k_A and k_B:

$$A + X \xrightarrow{k_A} \text{products} \quad (1)$$

$$B + X \xrightarrow{k_B} \text{products} \quad (2)$$

Assuming that there are no loss processes other than these reactions and that there are no other processes producing the reactants, the following relation is valid:

$$\ln\left\{\frac{[A]_0}{[A]_t}\right\} = \frac{k_A}{k_B}\ln\left\{\frac{[B]_0}{[B]_t}\right\} \quad (3)$$

where $[A]_0$, $[A]_t$, $[B]_0$, and $[B]_t$ denote the concentrations of compounds A and B at times zero and t. A plot of $\ln([A]_0/[A]_t)$ versus $\ln([B]_0/[B]_t)$ will thus give the relative reaction-rate coefficient $\alpha = k_A/k_B$ as the slope, or in terms of the fractionation constant, $\epsilon = \alpha - 1$.

The experiments were carried out in a 250 L electropolished stainless steel smog chamber equipped with a White-type multiple reflection mirror system with a 120 m optical path length for rotovibrationally resolved infrared spectroscopy. The infrared spectra were recorded with a Bruker IFS 88 FTIR instrument equipped with a liquid-nitrogen-cooled InSb detector and an 1800−4000 cm^{-1} band-pass filter. At a nominal resolution of 0.125 cm^{-1}, 128 scans were co-added using boxcar apodization. Periods of data collection (ca. 10 min) were alternated with UV photolysis (ca. 1 min) until about 60% of the HCHO was consumed. For a given gas mixture, the entire experiment typically lasted 1.5 h. The reaction chamber was equipped with UV photolysis lamps mounted in a quartz tube inside the chamber, and all of the experiments were carried out in synthetic air (99.9990% purity AGA; CO and NO_x < 100 ppb) at 298 ± 2 K and 1013 ± 10 mbar. The temperature was monitored on the outside of the chamber, and it remained constant for the duration of the experiments. Before the experiments were carried out, the chamber was cleaned by photolyzing O_3 in the presence of water vapor to eliminate impurities in the system.

HCHO. The HCHO isotopomers used were in the form of paraformaldehyde, $(CH_2O)_n$. DCDO (99 at. % D) was obtained as paraformaldehyde from Isotech. $H^{13}CHO$ (99.8 at. % ^{13}C) was obtained from Aldrich as a formalin solution, which was freeze-dried to isolate the polymer. HCHO was obtained from Merck, and this chemical was also used to synthesize the $HCH^{18}O$ by exchange with $H_2{}^{18}O$ (95 at. % ^{18}O, from Campro Scientific). The monodeuterated formaldehyde was prepared from deuterated bromoform.[24] The paraformaldehyde samples were heated to produce gaseous formaldehyde monomers and flushed into the reaction chamber with synthetic air via a Pyrex gas-handling system. The pressures of the reactants were measured in a standard volume on the gas line using a 10 mbar range capacitance manometer. After the introduction of all of the reagents, the chamber was filled to 1013 mbar with synthetic air.

OH. OH radicals were generated by photolysis of isopropyl nitrite (IPN-H_6) or isopropyl nitrite-1,1,1,3,3,3-d_6 (IPN-D_6), which were synthesized from isopropyl alcohol and isopropyl alcohol-1,1,1,3,3,3-d_6, respectively. The deuterated compound was used to minimize overlap in the spectral region where most of the formaldehyde isotopomers absorb (2670−2880 cm^{-1}). However, some of the experiments were carried out using IPN-H_6, as well, to determine if the decomposition of IPN produces HCHO or DCDO. No differences in the KIEs between the two OH precursors were seen (see also D'Anna et al. for details).[18] These compounds were photolyzed using Philips TLD-08 fluorescence lamps ("black lamp", $\lambda_{max} \sim 370$ nm).

Cl and Br. The chlorine and bromine atoms were generated by photolysis of Cl_2 and Br_2 using the Philips TLD-08 fluorescence lamps. In this wavelength region, the Cl and Br atoms produced were in the ground state. The Cl_2 and Br_2 were standard laboratory-grade compounds and were purified by two freeze−pump−thaw cycles prior to use.

NO_3. The NO_3 radicals were generated inside the chamber by the thermal decomposition of N_2O_5. N_2O_5 was prepared by mixing a gas stream of NO_2 with excess O_3 and trapping the product at −78 °C. The N_2O_5 was subsequently purified by vacuum distillation.

Each of the four experiments (OH, Cl, Br, and NO_3) was carried out twice for three different mixtures of formaldehyde isotopomers: HCHO + DCDO, HCHO + HCDO, and HCHO + $H^{13}CHO$ + $HCH^{18}O$. The initial mixing ratios of the radical precursors were 2.0 ppm for Cl_2 and Br_2 and 20 ppm for N_2O_5 and IPN/IPN-D_6. The initial mixing ratio of each formaldehyde isotopomer was 0.5 ppm, giving a maximum ratio of 1.5 ppm formaldehyde in some of the experiments. The mixing ratio of formaldehyde was kept as low as possible to minimize interfering reactions (see below).

The experimental spectra have been analyzed using a global FTIR nonlinear least-squares spectral-fitting procedure (NLM) developed by D. W. T. Griffith.[25] This method simulates the spectrum of the mixture of the absorbing species from the initial concentrations of the absorbing species and, then, iterates to minimize the residual between the measured and simulated spectra. In the spectrum calculation, true absorption coefficients from the HITRAN[26] database are used if available; otherwise, a high-resolution measured spectrum can be used as a good approximation. A least-squares minimum residual between the measured and simulated spectra is typically achieved after 5−10

TABLE 1: Wavenumber Regions and Compounds Included in Fitting the Experimental Spectra[a]

HCHO isotopomer mixture	spectral regions analyzed (cm^{-1})	compounds included in spectral fitting
HCHO, DCDO	2670−2855, 2010−2190	HCHO, NO_2, HCl, HBr, DCDO, CO, CO_2, H_2O
HCHO, HCDO	2670−2855	HCHO, HCDO, NO_2, HBr, HCl
HCHO, $H^{13}CHO$, $HCH^{18}O$	2670−2855	HCHO, $H^{13}CHO$, $HCH^{18}O$, NO_2, HBr, HCl

[a] NO_2 was formed as a byproduct of N_2O_5 decomposition in the NO_3 reaction experiments.

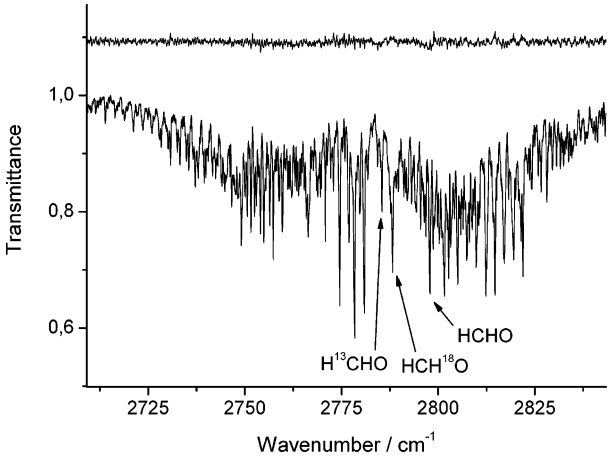

Figure 1. Example of a fitted spectrum of HCHO, $H^{13}CHO$, and $HCH^{18}O$ in the 2670−2855 cm^{-1} region. Lines corresponding to each isotopomer are indicated in the spectrum. The residual of the fit is shown above the spectrum. The correlation between the concentrations, derived by the least-squares fit of the spectra, is in all cases less than −0.1.

iterations, and the maximum correlation between the derived concentrations is −0.1.

The spectral features used in the analysis were the C−H stretching bands in the 2670−2855 cm^{-1} region and the C−D stretching bands in the 2010−2190 cm^{-1} region. The compounds considered in each spectral region are given in Table 1. The spectral data needed for the fitting procedure were taken from the HITRAN database (HCHO, CO, CO_2, HCl, HBr, and H_2O); for DCDO, HCDO, $H^{13}CHO$, and $HCH^{18}O$, experimental high-resolution IR spectra were used. These spectra were recorded with a Bruker IFS 120 FTIR instrument at a 0.01 cm^{-1} resolution in a 10 cm Pyrex gas cell equipped with CaF_2 windows. The partial pressures of formaldehyde isotopomers were in the range of 6−10 mbar, and the cell was filled to 1013 mbar with synthetic air (Air Liquide, dry technical air). The gas cell was passivated with ammonia before use to minimize the acid-catalyzed polymerization of the compound on the walls. A Ge on KBr beam splitter and an 1800−4000 cm^{-1} band-pass filter were used in the interferometer, and a glow bar (SiC_2) was used as the MIR light source. The detector was a liquid-N_2-cooled InSb semiconductor, and 128 scans were co-added to achieve an acceptable signal/noise ratio in the resultant spectra. An example of the fitted spectra of HCHO, $H^{13}CHO$, and $HCH^{18}O$ and the residuals of the fit are shown in Figure 1. The FTIR spectra showed accurate values for the relative change in concentrations. The data were analyzed according to eq 3 using a weighted least-squares procedure, which includes uncertainties in both reactant concentrations.[27] That is, the least-squares regression was carried out without allowing a zero-point offset, with the point (0,0) being the calibration or anchor point.

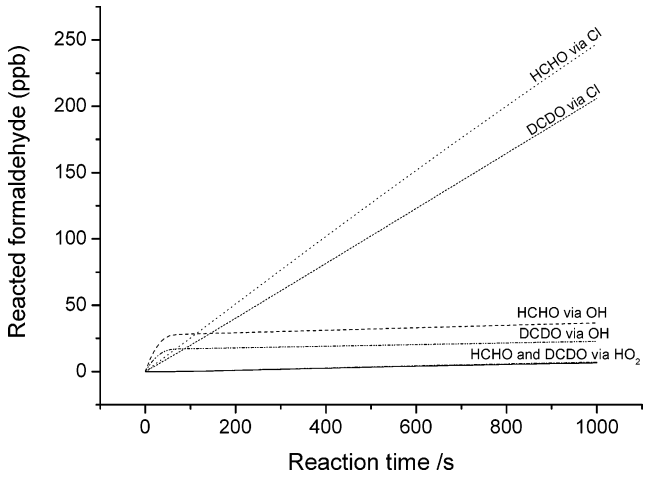

Figure 2. FACSIMILE model showing the maximum contributions from OH and HO_2 radical reactions in a Cl/HCHO/DCDO experiment. The halogen and NO_3 experiments are potentially susceptible to error because of the OH and HO_2 generated photochemically in the reaction chamber. This scenario shows that, with the initial concentrations used in this study, the OH reaction is significant during the first 70 s of photolysis and becomes negligible thereafter. The worst-case scenario is a 2% contribution to the relative rates from OH and HO_2 radicals.

Results and Discussion

The reactions of OH, Cl, Br, and NO_3 radicals with formaldehyde can proceed in three possible ways:

$$X + HCHO \rightarrow H + XCHO \quad (1a)$$

$$\rightarrow HX + HCO \quad (1b)$$

$$\rightarrow HX + H + CO \quad (1c)$$

The substitution reaction (eq 1a) is negligible.[18,19] In the presence of O_2, reactions 1b and 1c rapidly lead to CO and HO_2 production. HO_2 is a potential source of error as it reacts with formaldehyde to form an adduct, $HOO-CH_2-O$.[28] This adduct further reacts to form HCOOH and other products (see refs 18 and 19). In the case of the NO_3 experiments, HO_2 can also react with NO_3 to produce OH radicals: $HO_2 + NO_3 \rightarrow NO_2 + O_2 + OH$ ($k = 3.5 \times 10^{-16}$ cm^3 s^{-1}).[29] Since the reaction of NO_3 with formaldehyde is orders of magnitude slower than the OH reaction (5.6×10^{-16} cm^3 s^{-1} compared to 9.4×10^{-12} cm^3 s^{-1}),[9] this is a potential source of error. In addition, the presence of NO_x in the synthetic air (<100 ppb) means that O_3 and OH will be formed during the photochemical halogen reactions. The reaction system was therefore examined in a FACSIMILE[30] kinetic model employing 89 reactions (published as supporting material in Beukes et al.[19]) in order to elucidate the extent of competing chemical reactions. The model showed that the amount of formaldehyde that reacts with HO_2 is strongly dependent on the initial concentration of formaldehyde. Figure 2 shows the worst-case scenario for a chlorine experiment with 1.5 ppm formaldehyde and 100 ppb NO_x in the cell. The OH reaction is significant during the first 70 s of the reaction, and beyond that point, the chlorine reaction dominates completely. On the basis of this model, a maximum of 2% formaldehyde reacts with something other than chlorine. A similar scenario was observed for the Br reaction. Following the model results, we did not include data from the first 70 s of photolysis in the Cl and Br experiments. The model of the NO_3 experiment shows a 1% contribution to the HCHO degradation from OH. The

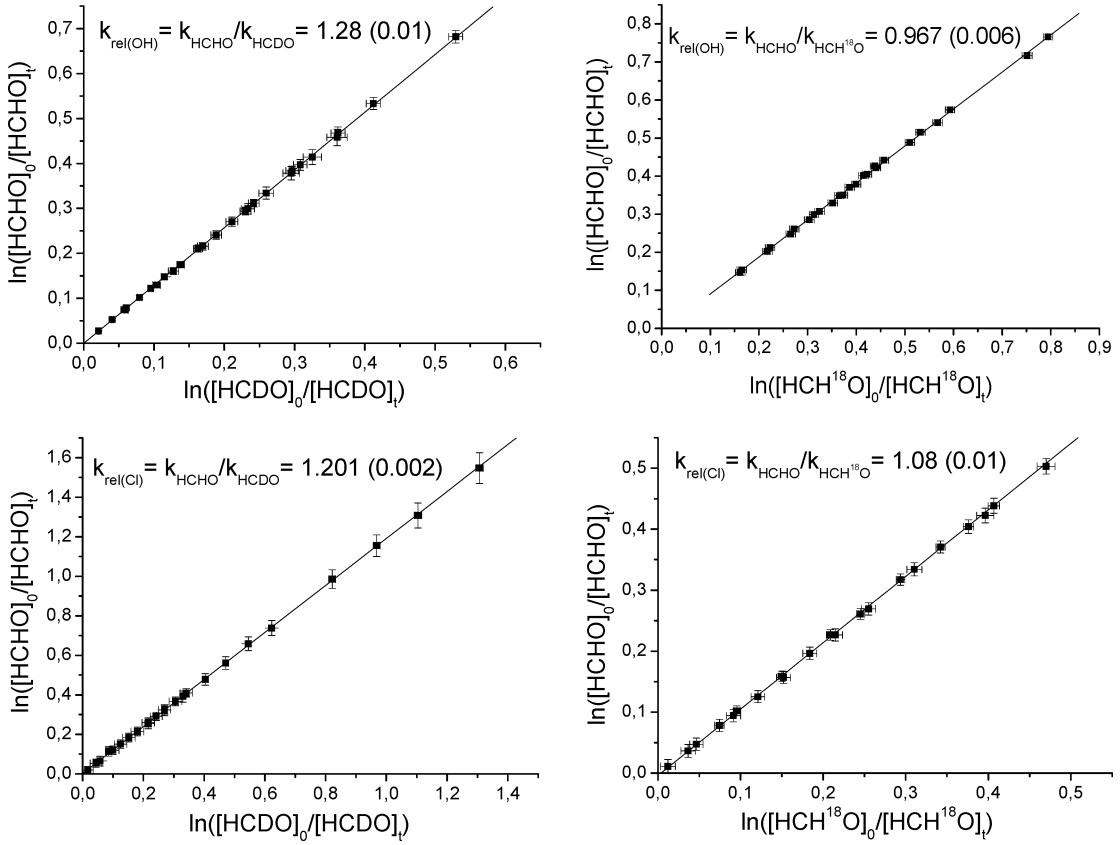

Figure 3. Plots of $\ln([HCHO]_0/[HCHO]_t)$ vs $\ln([HCDO]_0/[HCDO]_t)$ and $\ln([HCH^{18}O]_0/[HCH^{18}O]_t)$ during the reactions with OH and Cl radicals. Each plot contains data from two independent experiments with a total of at least 15 data points. The uncertainty assigned to each data point is 2σ statistical error from the spectral-fitting procedure and does not include possible systematic errors. The results are summarized in Table 2.

model also indicates that about 18 ppb formic acid will form during the reactions, which is below the detection limit of the experiment (a spectral window of 1800−4000 cm^{-1}). Indeed, it was not observed in the spectra during any of the experiments.

The relative-rate plots, $\ln([A]_0/[A]_t)$ versus $\ln([B]_0/[B]_t)$, for the HCDO and $HCH^{18}O$ experiments are shown in Figures 3 and 4. The plots include two independent experiments with a total of at least 15 data points for each experiment. The results of all of the experiments are summarized in Table 2. The relative reaction rates of HCHO, DCDO, and $H^{13}CHO$ with the four radicals have been studied previously by this group, and the results obtained in the present study are in excellent agreement with the earlier work, with the exception of the $k_{Br+HCHO}/k_{Br+DCDO}$ relative rate.[18,19] Niki and co-workers[22] have reported a value of 1.35 ± 0.15 for $k_{Cl+HCHO}/k_{Cl+DCDO}$ that is in agreement with our results. In a separate study, the same group found no KIE outside experimental error for the OH reaction with H^{13}-CHO.[22,23] There is a difference outside experimental error between the previous and present results for the $k_{Br+HCHO}/k_{Br+DCDO}$ ratio; this is likely due to inaccuracies in the standard spectral subtraction procedure used in the previous study and caused by insufficient spectral resolution.[19] There is one previous study of the $k_{OH+HCHO}/k_{OH+HCDO}$ ratio by Morris and Niki that uses mass spectrometry; however, they were not able to detect an isotope effect.[21] Modified RRKM calculations predict a $k_{OH+HCHO}/k_{OH+HCDO}$ KIE value of 1.34, which agrees very well with the KIE value of 1.284 ± 0.004 found in this study.[18] There are no previous studies to compare with our results for $HCH^{18}O$.

There are two clear trends in the KIEs in Table 2. One obvious trend is that deuteration generally leads to larger isotope effects than substitution by a heavy isotope of C or O; the other is that the halogens lead to significantly larger KIEs than OH and NO_3. It is straightforward to argue that deuteration should affect the reaction rate the most since it corresponds to the largest relative change in mass and involves the active site in the reaction. The reactions of formaldehyde with OH, Cl, Br, and NO_3 are all known to proceed via hydrogen abstraction in atmospheric conditions, and the C−O bond is passive in this context.[18] Substituting with deuterium also reduces the tunneling of the hydrogen. This is likely to have some effect on the reaction rate of the Br reaction, where there is a significant barrier for hydrogen to leave the system. For the OH, Cl, and NO_3 reactions, the barriers are small and tunneling is unlikely to play a major role.

One of the origins of the kinetic isotope effect is the change in zero-point energy (ZPE) brought about by isotopic substitution; the large KIEs in the halogen reactions are mainly due to zero-point vibration effects. The KIEs of the deuterated compounds are larger than can be explained by changes in ZPE; it is likely that quantum mechanical tunneling effects need to be taken into account. The changes in ZPE may however account for the KIEs in the reactions of $HCH^{18}O$ and $H^{13}CHO$ with the halogens. The KIEs for the reactions of $HCH^{18}O$ and $H^{13}CHO$ with OH and NO_3 radicals are inverse KIEs; for example, the heavy isotopomer reacts faster than the light isotopomer. This is an interesting effect, the origin of which might lie in the known formation of prereaction adducts in which the carbonyl oxygen is oriented toward the radical species. Quantum chemical calculations suggest that the OH−HCHO adduct is more stable and longer lasting than the Cl/Br−HCHO adducts, which means that the energetics of the adduct play an overall greater part in the KIEs of the OH reaction.[18,19] The preadduct of the reaction involves a bond between the OH hydrogen and the carbonyl oxygen in HCHO, which means that

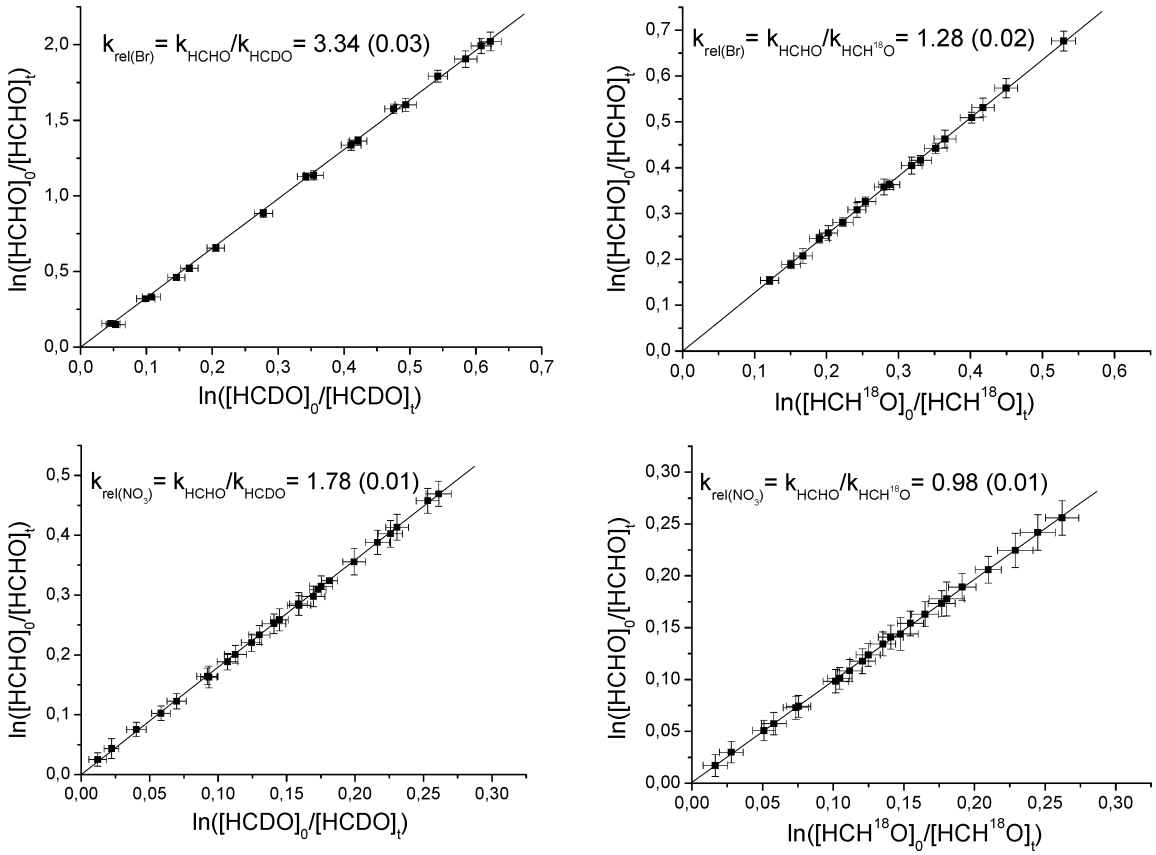

Figure 4. Plots of $\ln([HCHO]_0/[HCHO]_t)$ vs $\ln([HCDO]_0/[HCDO]_t)$ and $\ln([HCH^{18}O]_0/[HCH^{18}O]_t)$ during the reactions with Br and NO_3 radicals. Each plot consists of two independent experiments with a total of at least 15 data points. The uncertainty assigned to each data point is 2σ statistical error from the spectral-fitting procedure and does not include possible systematic errors. The results are summarized in Table 2.

TABLE 2: Relative Reaction Rates of Formaldehyde Isotopomers Given as $\alpha = k(X + H_2CO)/k(X +$ isotopomer)[a]

HCHO/isotopomer	α(OH) 9.4×10^{-12} [b]	α(Cl) 7.3×10^{-11} [b]	α(Br) 1.2×10^{-13} [b]	α(NO_3) 5.6×10^{-16} [b]
HCHO/DCDO	1.64 (0.01)	1.32 (0.01)	6.6 (0.1)	3.01 (0.02)
	1.67 (0.01)	1.30 (0.01)	6.8 (0.1)	3.04 (0.02)
	1.66 (0.01)	**1.31 (0.01)**	**6.7 (0.1)**	**3.02 (0.01)**
ref values	1.62 (0.05)[c]	1.302 (0.014)[d]	7.5 (0.2)[d]	2.97 (0.09)[c]
		1.35 (0.15)[e]		
HCHO/HCDO	1.28 (0.01)	1.203 (0.002)	3.33 (0.05)	1.77 (0.02)
	1.29 (0.01)	1.191 (0.006)	3.25 (0.04)	1.79 (0.02)
	1.28 (0.01)	**1.201 (0.002)**	**3.27 (0.03)**	**1.78 (0.01)**
ref values	~1[f]			
HCHO/H^{13}CHO	0.961 (0.008)	1.06 (0.01)	1.12 (0.01)	0.95 (0.01)
	0.95 (0.01)	1.051 (0.009)	1.14 (0.01)	0.96 (0.01)
	0.952 (0.005)	**1.058 (0.007)**	**1.13 (0.01)**	**0.96 (0.01)**
ref values	0.97 (0.03)[c]	1.07 (0.03)[d,g]	1.103 (0.03)[d,h]	0.97 (0.03)[d]
	1.1 (0.4)[i,j]			
HCHO/$HCH^{18}O$	0.972 (0.008)	1.07 (0.01)	1.26 (0.01)	0.98 (0.01)
	0.960 (0.009)	1.08 (0.01)	1.278 (0.008)	0.99 (0.01)
	0.967 (0.006)	**1.08 (0.01)**	**1.275 (0.008)**	**0.98 (0.01)**

[a] The weighted mean is given in bold. Errors represent 2σ from the statistical analyses and are given in parentheses. [b] Absolute rate constant at 298 K (ref 9). HCHO + X (cm^3 s^{-1}). [c] From ref 18. [d] From ref 19. [e] From ref 22. [f] From ref 21. [g] Calculated from the relative rates $k_{Cl+HCHO}/k_{Cl+DCDO}$ and $k_{Cl+H^{13}CHO}/k_{Cl+DCDO}$. [h] Calculated from the relative rates $k_{Br+HCHO}/k_{Br+DCDO}$ and $k_{Br+H^{13}CHO}/k_{Br+DCDO}$. [i] From ref 23. [j] Calculated from the relative rate $k_{Cl+H^{13}CHO}/k_{Cl+C_2H_4}$.

the stability of the complex is directly affected by isotopic substitution in the carbonyl group. The NO_3-HCHO adduct energy has not been calculated correctly; the electronic structure of the NO_3 radical presents a challenge to theoreticians due to symmetry breaking, and at present, there is no standard size extensive method applicable to larger systems.[31] Inverse isotope effects are also seen in the reaction of CO with OH, which is a complex-forming reaction.[32,33]

For stratospheric applications, it is necessary to consider a possible temperature dependence of the KIEs in these reactions. A significant temperature dependence of the total reaction rate has been reported for the Br reaction; the OH reactions have little or no temperature dependence, which may be attributed to the lack of a reaction barrier for these reactions.[9] The temperature dependence of the NO_3 reaction has not been quantified, but since the Arrhenius activation energy is low, it

is likely to be small. On the basis of the assumption that the KIE does not change significantly with temperature if the total rate does not change, only the KIE for the Br reaction may need to be corrected at stratospheric temperatures.

Conclusion

We report new data on the isotopic signatures of the reactions of five isotopomers of HCHO with OH, Cl, Br, and NO_3. These reactions exhibit distinct, measurable isotope effects containing information on the reaction potentials, which are useful for constructing atmospheric isotope budgets. The deuterium isotope effects are the largest, which might be expected since the reactions in question involve hydrogen abstraction and because deuteration represents the largest relative change in mass. In all of the cases, the active bonds in the reactions are the C−H and C−D bonds. Bromine shows the largest isotope effects, particularly for HCDO and DCDO, which may be attributed to zero-point vibration effects. It is interesting to note that the isotope effects for $H^{13}CHO$ and $HCH^{18}O$ and their reactions with OH and NO_3 are inverse kinetic isotope effects; for example, they react faster than HCHO with these radicals. We attribute this to prereaction adduct formation involving the carbonyl group. The most important KIEs with respect to the atmosphere are the those of HCDO, $H^{13}CHO$, and $HCH^{18}O$ in the OH and Cl reactions. The carbon and oxygen isotopic signature in formaldehyde is propagated to CO, which is known to be enriched in heavy isotopes of oxygen and carbon. These relative rates can therefore be important pieces of information when tracing the isotopic enrichment of CO.[13,34] Both the $k_{OH+HCHO}/k_{OH+HCDO}$ KIE, which is most important in the troposphere, and the $k_{Cl+HCHO}/k_{Cl+HCDO}$ KIE, which is significant in the stratosphere, lead to a large enrichment of deuterium in the remaining formaldehyde and, in turn, a deuterium enrichment in atmospheric molecular hydrogen.

Acknowledgment. The experiments were made possible by a researcher mobility grant from the Nordic Network for Chemical Kinetics supported by the Nordic Academy for Advanced Study (NorFA) and by the financial support of the Danish Natural Science Research Council. The authors thank Else Philipp for her valuable assistance with the synthesis of formaldehyde isotopomers, David W. T. Griffith for providing us with the spectral fitting method, and Flemming M. Nicolaisen for his help with recording the high-resolution spectra.

References and Notes

(1) Houghton, J. T., Ding, Y., Griggs, D. J., Noguer, M., van der Linden, P. J., Dai, X., Maskell, K., Johnson, C. A., Eds. *Climate Change 2001: The Scientific Basis*, IPCC, Working Group I to the Third Assessment Report of the Intergovernmental Panel on Climate Change, 2001; Cambridge University Press: Cambridge, U.K., 2001.

(2) Sumner, A. L.; Shepson, P. B.; Couch, T. L.; Thornberry, T.; Carroll, M. A.; Sillman, S.; Pippin, M.; Bertman, S.; Tan, D.; Faloona, I.; Brune, W.; Young, V.; Cooper, O.; Moody, J.; Stockwell, W. *J. Geophys. Res.* **2001**, *106*, 24387.

(3) Anderson, L. G.; Lanning, J. A.; Barrel, R.; Miyagishima, J.; Jones, R. H.; Wolfe, P. *Atmos. Environ.* **1995**, *30*, 2113.

(4) Wagner, V.; von Glasow, R.; Fischer, H.; Crutzen, P. J. *J. Geophys. Res.* **2002**, *107*, 1.

(5) Fried, A.; Lee, Y. N.; Frost, G.; Wert, B.; Henry, B.; Drummond, J. R.; Hübler, G.; Jobson, T. *J. Geophys. Res.* **2002**, *107*, 4039.

(6) Wang, Y.; Ridley, B.; Fried, A.; Cantrell, C.; Davis, D.; Chen, G.; Snow, J.; Heikes, B.; Talbot, R.; Dibb, J.; Flocke, F.; Weinheimer, A.; Blake, N.; Blake, D.; Shetter, R.; Lefer, B.; Atlas, E.; Coffey, M.; Walega, J.; Wert, B. *J. Geophys. Res.* **2003**, *108*, 8358.

(7) Smith, G. D.; Molina, L. T.; Molina, M. J. *J. Phys. Chem. A* **2002**, *106*, 1233.

(8) Seinfeld, J. H.; Pandis, S. N. *Atmospheric Chemistry and Physics: From Air Pollution to Climate Change*; John Wiley & Sons: New York, 1998.

(9) Atkinson, R.; Baulch, D. L.; Cox, R. A.; Crowley, J. N.; Hampson, R. F., Jr.; Kerr, J. A.; Rossi, M. J.; Troe, J. Summary of Evaluated Kinetic and Photochemical Data for Atmospheric Chemistry. IUPAC Subcommittee on Gas Kinetic Data Evaluation for Atmospheric Chemistry, 2001.

(10) Allan, W.; Lowe, D. C.; Cainey, J. M. *Geophys. Res. Lett.* **2001**, *28*, 3239.

(11) Shepson, P. B.; Sirju, A. P.; Hopper, J. F.; Barrie, L. A.; Young, V.; Niki, H.; Dryfhout, H. *J. Geophys. Res.* **1996**, *101*, 21081.

(12) Barrie, L. A.; Bottenheim, J. W.; Schnell, R. C.; Crutzen, P. J.; Rasmussen, R. A. *Nature* **1988**, *334*, 138.

(13) Brenninkmeijer, C. A. M.; Jannsen, C.; Kaiser, J.; Röckmann, T.; Rhee, T. S.; Assonov, S. S. *Chem. Rev.* **2003**, *103*, 5125.

(14) Rahn, T.; Eiler, J. M.; Boering, K. A.; Wennberg, P. O.; McCarthy, M. C.; Tyler, S.; Schauffler, S.; Donnell, S.; Atlas, E. *Nature* **2003**, *424*, 918.

(15) Hauglustaine, D. A.; Ehhalt, D. H. *J. Geophys. Res.* **2002**, *107*, 4330.

(16) Prather, M. J. *Science* **2003**, *302*, 581.

(17) Schultz, M. G.; Diehl, T.; Brasseur, G. P.; Zittel, W. *Science* **2003**, *302*, 624.

(18) D'Anna, B.; Bakken, V.; Beukes, J. A.; Nielsen, C. J.; Brudnik, K.; Jodkowski, J. T. *Phys. Chem. Chem. Phys.* **2003**, *5*, 1790.

(19) Beukes, J. A.; D'Anna, B.; Bakken, V.; Nielsen, C. J. *Phys. Chem. Chem. Phys.* **2000**, *2*, 4049.

(20) Beukes, J. A.; D'Anna, B.; Nielsen, C. J. *Asian Chem. Lett.* **2000**, *4*, 145.

(21) Morris, E. D., Jr.; Niki, H. *J. Chem. Phys.* **1971**, *55*, 1991.

(22) Niki, H.; Maker, P. D.; Breitenbach, L. P.; Savage, C. M. *Chem. Phys. Lett.* **1978**, *57*, 596.

(23) Niki, H.; Maker, P. D.; Savage, C. M.; Breitenbach, L. P. *J. Phys. Chem.* **1984**, *88*, 5342.

(24) Ouzounian, J. G.; Anet, F. A. L. *J. Labelled Compd. Radiopharm.* **1986**, *23*, 401.

(25) Griffith, D. W. T. *Appl. Spectrosc.* **1996**, *50*, 59.

(26) Rothman, L. S. *J. Quant. Spectrosc. Radiat. Transfer* **1998**, *60*, 665.

(27) York, D. *Can. J. Phys.* **1966**, *44*, 1079.

(28) Aloisio, S.; Francisco, J. S. *J. Phys. Chem. A* **2000**, *104*, 404.

(29) Mellouki, A.; Talukdar, R. K.; Bopagedera, A. M. R. P.; Howard, C. J. *Int. J. Chem. Kinet.* **1993**, *25*, 25.

(30) *FACSIMILE*; AEA Technology: 1998.

(31) Eisfeld, W.; Morokuma, K. *J. Chem. Phys.* **2000**, *113*, 5587.

(32) Weston, R. E., Jr. *J. Phys. Chem. A* **2001**, *105*, 1656.

(33) Feilberg, K. L.; Sellevåg, S. R.; Nielsen, C. J.; Griffith, D. W. T.; Johnson, M. S. *Phys. Chem. Chem. Phys.* **2002**, *4*, 4687.

(34) Röckmann, T.; Jöckel, P.; Gros, V.; Bräunlich, M.; Possnert, G.; Brenninkmeijer, C. A. M. *Atmos. Chem. Phys.* **2002**, *2*, 147.